PROTEINS: Structure, Function, and Genetics 29:426–432 (1997)

Highly Constrained Multiple-Copy Refinement of Protein Crystal Structures

Matteo Pellegrini,[1] Niels Grønbech-Jensen,[1,2] Jennifer A. Kelly,[1] Gaston M.U. Pfluegl,[1] and Todd O. Yeates[1]*
[1]*Molecular Biology Institute, University of California, Los Angeles, Los Angeles, California*
[2]*Theoretical Division, Los Alamos National Laboratory, Los Alamos, New Mexico*

ABSTRACT **In the course of refining atomic protein structures, one often encounters difficulty with molecules that are unusually flexible or otherwise disordered. We approach the problem by combining two relatively recent developments: simultaneous refinement of multiple protein conformations and highly constrained refinement. A constrained Langevin dynamics refinement is tested on two proteins: neurotrophin-3 and glutamine synthetase. The method produces closer agreement between the calculated and observed scattering amplitudes than standard, single-copy, Gaussian atomic displacement parameter refinement. This is accomplished without significantly increasing the number of fitting parameters in the model. These results suggest that loop motion in proteins within a crystal lattice can be extensive and that it is poorly modeled by isotropic Gaussian distributions for each atom. Proteins 29:426–432, 1997.** © 1997 Wiley-Liss, Inc.

Key words: overdamped langevin dynamics; thermal motion; neurotrophin; glutamine synthetase; atomic displacement parameter; x-ray diffraction data; loop mobility; disorder

INTRODUCTION

The diffraction of x-rays from protein crystals allows crystallographers to model complex molecular structures at atomic resolution. Implicit in the vast majority of the models collected in the Protein Data Bank is that only a single conformational state contributes to the diffraction. Atomic motion is ordinarily modeled by a Gaussian distribution centered at each atomic position, whose width is fit to maximize the agreement between the data and the model.

In general, if the resolution of the data extends to approximately 1 Å, anisotropic Gaussian motion of the atoms can be modeled accurately (e.g., see Ref. 1). Limited resolution from most protein crystals restricts modeling to isotropic displacements.

The description of atomic thermal motion by Gaussian distributions assumes that each atom vibrates in a harmonic potential well. This assumption describes protein motion poorly, because the atomic vibrations in these polymers are highly coupled (as suggested by diffusely scattered x-rays[2]) and nonharmonic (as seen in side chains with multiple conformations in high-resolution structures). Nonetheless, the Gaussian motion model has proved to be highly effective in describing the scattering of many proteins.

As the science of protein crystallography advances, a greater number of cases emerge in which the crystal asymmetric unit accommodates a very large protein and/or a large number of proteins. Also, cases arise in which the motion of a moderately sized protein is not described well by the isotropic model. These situations require an alternative description of protein motion to achieve reasonable agreement with the diffraction data. One possibility is to describe the diffraction not as arising from a single conformation of the protein, but by an ensemble of several conformations.[3–7] Nuclear magnetic resonance experiments,[8] and computer simulations of protein motions[9] suggest that proteins sample several conformations in solution. We show, as has been shown previously,[3,4,6] that even within the confines of a crystal lattice, some proteins are able to sample quite varied conformations.

We have collected data from crystals of two distinct proteins: a highly flexible protein, neurotrophin-3, and a glutamine synthetase dodecamer. In both cases we simultaneously refine 10 copies of the protein against the diffraction data. The final refined ensemble of structures shows significant conformational variation between the copies, suggesting that the variability is not described well by Gaussian distributions. The multiple-copy models lead to closer agreement between the observed and calculated data than single-copy models.

In our refinement procedure, a fully constrained algorithm moves the protein such that only main-chain ϕ-ψ dihedral angles and side-chain torsion angles are free to vary; this method is similar to

*Correspondence to: Todd O. Yeates, Molecular Biology Institute, University of California, Los Angeles, Los Angeles, CA 90095-1570.
Received 21 April 1997; Accepted 31 July 1997

torsion angle refinement described recently by Rice and Brunger.[10] Unlike previous work, the present study combines the constrained algorithm with multiple protein copies and includes a single Gaussian distribution width, identical for all atoms, to model rigid body motions. We test the algorithm on structures that have a high degree of disorder. These are poorly modeled by a single-protein copy, as suggested by high values of R and R_{free} after conventional refinement. The crystallographic R value is defined as

$$R = \sum_{h,k,l} \frac{|F_o(h, k, l) - F_c(h, k, l)|}{F_o(h, k, l)} \quad (1)$$

where $F_o(h, k, l)$ is the observed magnitude of the structure factor with Miller indices h, k, and l, and $F_c(h, k, l)$ is the structure factor calculated from the model. The R_{free}, calculated from approximately 10% of the data that is removed from the refinement, cross-validates the resulting model.[11]

Our constrained protein model contains approximately 3 degrees of freedom per residue, approximately one tenth the number for fully flexible models that have 3 positional degrees of freedom and one Gaussian width per atom. Therefore, the dimensionality of the parameter space associated with the two refinement methods is very similar if we use 10 copies in our method. However, the positional parameters in the single-copy refinement are highly restrained by potentials between atoms, as are the values of the Gaussian widths between bonded atoms. In contrast, our refinements impose no restraints between the values of the dihedral angles between copies. Although the dimensionality of the parameter space is similar, in our refinement the volume of accessible parameters within this space is probably larger. We are cautious in comparing R values obtained from the two methods and rely on cross-validation, using R_{free}, to ensure that the multiple-copy refinements are meaningful and not simply overfitting the data.

MATERIALS AND METHODS

Because 10 protein copies are typically refined simultaneously, we compensate by limiting the number of free parameters by constraining bond lengths and angles to their ideal values. Main-chain ϕ-ψ dihedral angles and side-chain χ angles freely rotate. The constraints are imposed with a technique described below, used by Deutch and Madden[12] to simulate linear polymers and then applied to polyalanine by Grønbech-Jensen and Doniach.[13] The principal difference between this method and that introduced earlier by Rice and Brunger[10] is that here we solve an overdamped Langevin equation instead of an undamped dynamical equation.

The method entails solving a set of linear equations at each time step, to obtain the tension that each bond exerts on the bonded atoms. Once the tensions (t_j) are known, an overdamped Langevin equation gives the change in position of each atom:

$$\frac{\partial \boldsymbol{r}_i}{\partial \boldsymbol{t}} = \sum_j t_j(\boldsymbol{r}_j - \boldsymbol{r}_i) + \nu_i \quad (2)$$

The sum is over all atoms to which the ith atom is bonded, and ν_i is a force term that incorporates the observed diffraction information. The forces on the atoms are calculated from the gradients of the $F_o - F_c$ maps[14] plus a noise term. A Gaussian noise term is added to the forces. This sets the temperature scale and introduces a random element that allows different copies to undergo distinct trajectories. The tensions are computed by ensuring that the time derivatives of the constrained lengths are all zero:

$$(\boldsymbol{r}_j - \boldsymbol{r}_i) \cdot \frac{\partial(\boldsymbol{r}_j - \boldsymbol{r}_i)}{\partial \boldsymbol{t}} = 0. \quad (3)$$

The tensions may be extracted after inserting Eq. (2) into Eq. (3).

To preserve the angle between two bonds, a constraint is imposed between the two nonbonded atoms in the triplet. Similarly, to preserve the planarity of three bonds, dummy atoms are introduced and constrained a fixed distance from the four atoms in the plane.

We initially impose a single isotropic Gaussian atomic displacement factor that is the same for all atoms. The positional displacements calculated from the $F_o - F_c$ maps are multiplied by a constant to obtain a force. This constant is chosen, together with the time step of the integrator, to preserve the constrained lengths at each time step to within 0.001 Å. During the course of refinement, bond lengths typically do not drift by more than 0.01 Å.

To maximize the convergence of the refinement, the magnitude of the noise term is set to approximately one tenth the magnitude of the force term due to the diffraction information. The simulation contains no other force terms, such as nonbonded interactions. Intramolecular van der Waals forces are excluded because we are describing an ensemble of structures for which these forces are not well defined.

RESULTS

Neurotrophin-3

Neurotrophin-3 (NT-3) is one of the four proteins that comprise the neurotrophin family, a group of growth factors that controls the development and maintenance of neurons. Two neurotrophin structures have previously been published: the murine nerve growth factor (NGF) homodimer[15,16] and the

Table I. Variation of *R* Values vs. Number of Copies for NT-3 Constrained Refinement

No. of copies	R	R_{free}
5	21.6	37.3
10	17.7	35.1
20	17.7	35.2

human brain-derived neurotrophic factor (BDNF) and NT-3 heterodimer.[17] The proteins consist of approximately 118 residues forming a curved β-sheet. Both structures contain ill-defined loops (residues 42–48 and 59–74) and have high overall atomic displacement factors (34 and 45.8 Å^2).

We obtained recombinant NT-3 from Amgen.[18] The crystals were grown in 12% polyethylene glycol, 0.5 M sodium citrate, and 15% dimethyl formamide at pH 5.0. The crystals formed space group $P2_12_12$ and diffracted to 2.6 Å. The diffraction data were collected at line X12-C of the National Synchrotron Light Source (NSLS). The unit cell dimensions were 37.97, 51.9, and 65.99 Å. The data set was 97% complete with an R_{merge} of 0.074 and and average I/σ of 3.78.

The initial phases were obtained from molecular replacement with the NGF dimer[16] as the starting model; by using X-PLOR[19] and AMoRe,[20] we obtained the same rotation function solutions. Single-copy refinement with isotropic Gaussian atomic displacements, using the program X-PLOR, produced a model with an R value of 28.4% and an R_{free} of 37.9% on data from 2.75 to 6.0 Å. No waters were included in the model because they did not significantly decrease the R values. Although the final R_{free} for this model is high, we have several indications that it represents an essentially correct solution: the same rotation function solution was obtained with different programs, the top solution was two standard deviations above the next best solution, and finally, the molecular replacement procedure was insensitive to the choice of starting models from the previously solved NGF, BDNF, or NT-3 crystals.

Starting from this partially refined model on NT-3, we attempted multiple-copy, constrained refinement with different numbers of copies, as shown in Table I. With respect to 10 copies, the R and R_{free} values were slightly higher for five copies and remained virtually unchanged for 20 copies. To optimize the speed and results, we used 10 copies for the subsequent refinements.

Compared with the standard single-copy refinement, our 10-copy refinement generates a model with a lower R_{free} value, 35.1%, and a significantly lower R value, 17.7%. Main-chain traces of the 10 copies, shown in Figure 1, illustrate disordered loops and consistent atom positions in the center of the four antiparallel β-strands. This is qualitatively similar to what is observed when the three previous crystal structures of neurotrophin are superimposed.[17]

Fig. 1. An α-carbon trace of NT-3. The 10 copies were refined simultaneously under strict geometrical constraints.

We chose a value of 20 Å^2 for the single atomic displacement parameter used in this (and all subsequent) refinements. The R values are reported after approximately 5,000 steps of Langevin dynamics. Fast Fourier transforms were recalculated when the maximum displacement of an atom exceeded 0.2 Å.

The constrained multiple-copy and standard single-copy refinement techniques have a similar number of free parameters. The NT-3 data-to-parameter ratio in both cases is 1.1, neglecting the effects of restraints in standard refinement. However, our method has a higher accessible volume of parameter space because the values of the dihedral angles are not restrained. Therefore, it might be misleading to compare our value of R with that obtained from the single-copy Gaussian refinement. However, the decrease in the R_{free} value suggests that the multiple-

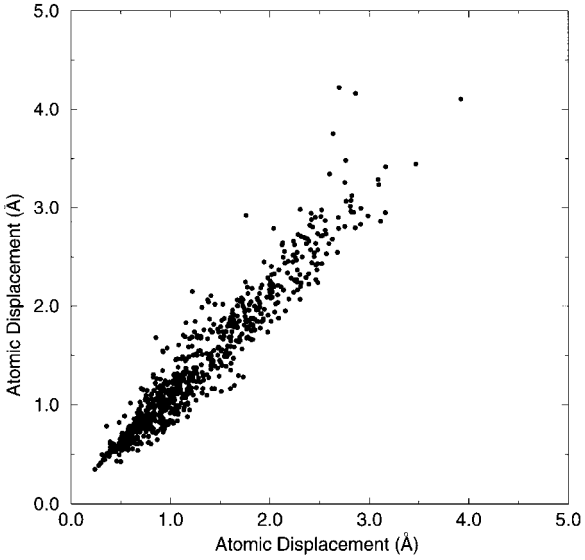

Fig. 2. A comparison of atomic positional variation in two independent multiple-copy refinements. The positional variation is defined as the root mean square deviation from the average position for equivalent atoms in the 10 simultaneously refined copies of the molecules. We plot these distances for all atoms in neurotrophin-3 obtained at the end of two refinement runs. The correlation coefficient is 0.97.

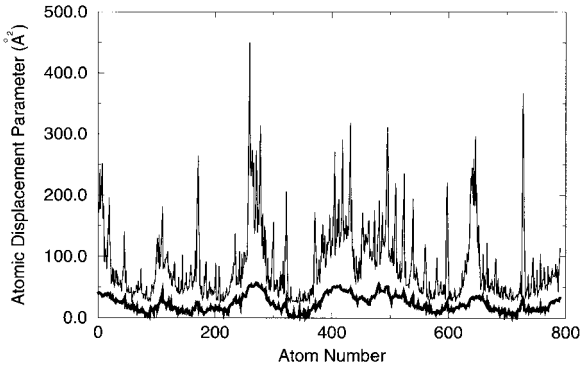

Fig. 3. A comparison of positional variation in multiple-copy refinement (thin line) and standard isotropic atomic displacement parameter (thick line) as a function of atom number. For the multiple-copy refinement the positional variation is defined as $8\pi^2/3$ times the root mean square deviation from the average position for equivalent atoms in the 10 simultaneously refined copies of the molecules, plus the uniform isotropic displacement parameter. The thin line represents the atomic displacement parameters that describe isotropic Gaussian motion in standard single-copy refinement. The values are plotted for all nonhydrogen atoms in NT-3.

copy model is more accurate. If the loop motion contained in the multiple models is approximately correct, it is not surprising that a single copy is unable to model such extensive conformational variation.

To assess the uniqueness of these refinement runs, the NT-3 refinement was repeated several times with different seeds for the random number generator. We evaluate the positional variation in each atom among the 10 copies and compare this variation between two independent runs. We compute the standard linear correlation

$$C = \frac{\sum_i rms_i^a rms_i^b}{\left(\sum_i (rms_i^a)^2 \sum_i (rms_i^b)^2\right)^{1/2}} \quad (4)$$

where a and b are the models obtained from two runs with different seeds, and rms_i is defined as the root mean square deviation of the 10 copies of atom i from their centroid. The correlation yields a value of 0.97 between two runs, as seen in Figure 2. Although the distribution of states obtained by multiple-copy refinement seems highly reproducible, the atomic positions are not exactly reproduced. The R values between two composite models (each consisting of 10 structures) are approximately 15%.

We also compare the root mean square atomic displacement between identical atoms in different copies to the atomic displacement parameters obtained from the standard single-copy Gaussian refinement. A superposition of displacement as a function of residue number is shown in Figure 3. The 0.85 linear correlation between these displacements indicates a high similarity between the pattern of disorder modeled by the two methods. However, it is clear from the figure that the displacement is found to be far greater in the multiple-copy model than in the single-copy one: the effective average atomic displacement parameter is 84.5 Å^2 for the multiple-copy model and 23.2 Å^2 for the single-copy, isotropic displacement. The lower values of R and R_{free} suggest that the disorder in NT-3 crystals is more accurately described by the multiple-copy models. This implies that isotropic atomic displacements may account for only a fraction of the overall disorder in some protein crystals.

We believe that our model provides a more physical picture of disorder than standard isotropic Gaussian models. The weak electron density and large displacement parameters suggest that the loops in NT-3 are disordered. The lower R values indicate that the conformational variation of the loops among multiple copies better describes the distribution of protein states within the crystal lattice than the isotropic vibration approximation.

Glutamine Synthetase

Glutamine synthetase (GS) is a key enzyme in nitrogen metabolism; it catalyzes the biosynthesis of glutamine from ammonia, glutamate, and ATP. GS from the bacterium *S. typhimurium* is a stable complex, consisting of 12 identical chains each of 468

amino acid residues, assembled in a dodecamer with D_6 symmetry (molecular weight 620 kd[21]).

GS expressed in *E. coli* was isolated by ammonium sulfate precipitation followed by a Cibachrom blue affinity column, as described earlier.[22] GS crystals were grown by the hanging drop method of vapor diffusion.[23] In the presence of ADP, GS crystallizes in space group C2 with 1 dodecamer per asymmetric unit with cell dimensions 234.5, 133.9, and 196.8 Å and $\beta = 101.2°$. Data were collected from a single crystal using synchrotron radiation at the NSLS beamline X12-C under cryogenic conditions with 30% MPD as cryoprotectant. The data set is 98% complete to 2.5 Å resolution, with 200,000 unique reflections, a 10-fold redundancy and an R_{merge} of 7.5%.

A 2.8 Å room temperature model,[24] obeying strict 12-fold noncrystallographic symmetry, was used as an initial model for molecular replacement. Conventional, single-copy refinement with isotropic displacement parameters, implemented by using the program X-PLOR,[19] was attempted both with noncrystallographic symmetry (NCS) constraints and without, against the 2.5 Å data set. With standard refinement the data-to-parameter ratio is 11 with NCS, and 0.9 without NCS constraints, neglecting the effects of geometrical restraints. Releasing the NCS constraints led to an increase in the value of R_{free}, suggesting that the data were insufficient to model all 12 monomers independently. In the case where a single monomer copy was refined with NCS constraints, we obtain an R of 30.3% and an R_{free} of 31.9%. The refinement was performed with data from 8.0 to 2.5 Å. No water molecules were included in the model. Further details on the conventional refinement and a description of the GS structure will be presented elsewhere.

In the present study we refined 10 highly constrained copies of the GS monomer, maintaining the strict NCS constraints of the D_6 dodecamer. In this case, the variability of the model conformations arises from two factors: 1) the ensemble of conformations of monomers in a specific position in the dodecamer and 2) the ensemble of conformations of the monomers at different positions in the dodecamer.

Refinement with 10 copies of the molecule produced an R of 25.9% and an R_{free} of 29.4%. As seen in Figure 4, the outer regions of the dodecamer are highly variable, whereas the 10 models overlap closely in the inner portion.

We confirmed that the same results may be obtained by using the program X-PLOR.[19] The program was operated in the torsional refinement mode by using a single atomic displacement parameter, identical for all atoms. The final R and R_{free} values were 25.4 and 29.3%, respectively.

We also ran X-PLOR with 12 simulated annealing copies, instead of the torsional refinement mode, with a fixed atomic displacement of 31 for all atoms. In this case the R and R_{free} dropped even further to 21 and 26%. We believe this is in part due to the maintenance of strict NCS constraints. Previous work by Burling and Brunger[4] with penicillopepsin showed that when multiple copies with flexible bonds are refined simultaneously in the absence of NCS constraints, the R value may become extremely low (below 10%) even though the value of R_{free} stops falling. This indicates that the method leads to overfitting when more than eight flexible copies are used.

Fig. 4. The α-carbon trace of a glutamine synthetase monomer, refined using 10 highly constrained copies of the molecule.

We also attempted the highly constrained refinement with one copy per monomer and without NCS constraints between the molecules of the dodecamer and found that the R_{free} inevitably increases. The refinement conducted with one model copy and no NCS constraints has approximately the same number of unconstrained fitting parameters as the 10-copy, NCS-constrained refinement. The observation that the former leads to an increase in R_{free}, while the latter leads to a decrease, suggests that the 10-copy NCS-constrained model is generating a more accurate description of the scattering. Thus, the way one chooses to model disorder, and not simply the number of free parameters, is crucial to the outcome of the refinement.

Artificial Data

As a controlled test of the method, we evaluated how well an ensemble structure can be recovered in a case where the target actually consists of 10 conformations. Artificial diffraction data were generated from a 10-copy NT-3 model produced in an earlier refinement. The new algorithm was then used to refine an initial NT-3 model against the artificial data. The rms difference between the coordinates of the starting model and the centroid of the target ensemble was 0.8 Å. The initial R value was 35.7% for data between 2.5 and 10 Å resolution. The refinement decreased the R value to 9.1% and R_{free} to 9.8%. The rms difference between the centroid coordinates of the refined ensemble and the target ensemble dropped to 0.5 A, showing a net improvement in the centroid coordinates.

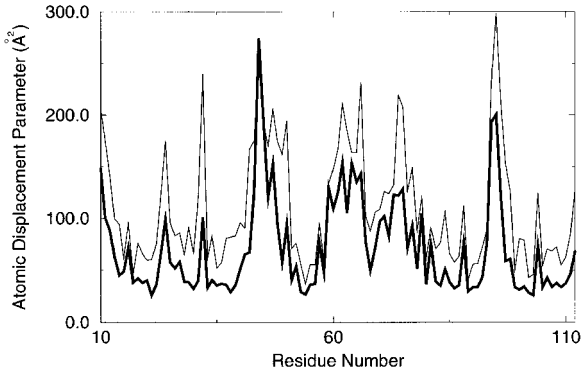

Fig. 5. A comparison of effective atomic displacement parameters in the model from which artificial diffraction data were calculated (thick line) vs. the refined ensemble of ten NT-3 molecules (thin line). The effective atomic displacement parameter is defined as $8\pi^2/3$ times the root mean square deviation from the average position for equivalent atoms in the 10 copies of the molecules. The values are averaged over the atoms in each residue.

The method was especially successful in describing the structural disorder. The effective atomic displacement parameters in the 10-copy NT-3 model from which the artificial data were calculated are compared in Figure 5 with the corresponding values for the refined model. Although the refinement captures the essential features of the disorder, it cannot reproduce the exact details of the disorder, as suggested by the residual discrepancy between the artificial data and the structure factors calculated from the final composite model and by the differences in atomic coordinates. This discrepancy affects the difference between the R and R_{free} values for the NT-3 refinement as discussed later.

By contrast, conventional single-copy refinement with isotropic atomic displacement parameters, using X-PLOR and the same artificial diffraction data, led to a higher final R value of 22.4%. The isotropic displacement parameters apparently capture only a small fraction of the disorder explicit in the test ensemble of 10 molecules.

CONCLUSIONS

Highly constrained multiple-copy refinements are reported for two proteins that exhibit a high degree of disorder, as suggested by the high atomic displacement factors and the high R and R_{free} values that were obtained from conventional single-copy refinement. In both cases the multiple copy refinement resulted in lower R and R_{free} values, without a significant increase in the number of fitting parameters.

Experimental data are usually accurate to better than 10%, as measured by the agreement between symmetry-related Bragg peaks. The NT-3 refinement results in an R_{free} greater than 30.0%, suggesting that the model falls short of a complete description of the scattering. Part of this discrepancy results from a failure to model the scattering from water.

The gap between R and R_{free} values in the NT-3 case probably arises from the fact that the disorder in the protein is not modeled uniquely by our method. We have shown that, although refinement runs with different seeds yield highly correlated mean atomic displacements, they do not yield identical structures. The R value between ensemble models in alternate runs is in the 15% range. The variability in final models accounts for some of the discrepancy between the R and R_{free} values.

Furthermore, we have shown that even with artificial data it is not possible to completely recover the correct ensemble of models. The final agreement between the artificial data and our refined model was slightly better than 10%. We therefore conclude that part of the discrepancy between R and R_{free} for NT-3 is due to the inability of our algorithm to reproduce the exact details of the structural disorder with the given data-to-parameter ratio.

In the other two examples, glutamine synthetase and NT-3 with artificial data, the discrepancy between R and R_{free} is much smaller. This is to be expected for artificial data, where the correct model is unambiguous. For the case of glutamine synthetase, the NCS constraints increase the data-to-parameter ratio by a factor of approximately 10 with respect to the NT-3 refinement, leading to a higher degree of correlation between refined models obtained with different starting seeds.

The present study introduces an alternate, and possibly more physically reasonable model for scattering in protein crystals by eliminating the fitting of isotropic Gaussian distribution widths for each atom in the molecule. A uniform atomic displacement factor value accounts for overall rigid body vibration, whereas multiple copies of the protein represent its distribution of states. Combining strict geometric constraints with multiple-copy refinement leads to a description of anisotropic disorder with a similar number of fitting parameters as conventional refinement with isotropic displacement parameters. By testing this approach on two disordered proteins, we achieve better agreement between the modeled and observed data than is possible with standard refinement.

ACKNOWLEDGMENTS

We thank Axel Brunger for useful comments on the manuscript. This work is supported by a Sloan Foundation, Department of Energy (DOE) postdoctoral fellowship (M.P.) and in part by the Associated Western Universities Inc. and DOE (J.K.). Portions of this work were conducted under the auspices of the DOE, supported by funds provided by the University of California to conduct discretionary research by Los Alamos National Laboratory (N.G.J.).

REFERENCES

1. Anderson, D.H., Weiss, M.S., Eisenberg, D. A challenging case for protein crystal structure determination: The mating pheromone Er-1 from Euplotes raikovi. Acta Crystallogr. D52:469–480, 1996.
2. Thune, T., Badger, J. Thermal diffuse X-ray scattering and its contribution to understanding protein dynamics. Prog. Biophys. Mol. Biol. 63:251–276, 1995.
3. Kuriyan, J., Osapay, K., Burley, S.K., Brunger, A.T., Hendrickson, W.A., Karplus, M. Exploration of disorder in protein structures by x-ray restrained molecular dynamics. Proteins 10:340–358, 1991.
4. Burling, F.T., Brunger, A.T. Thermal motion and conformational disorder in protein crystal structures: comparison of multi-conformer and time-averaging models. Isr. J. Chem. 34:165–175, 1994.
5. Burling, F.T., Weis, W.I., Flaherty, K.H., Brunger, A.T. Direct observation of protein solvation and discrete disorder with experimental crystallographic phases. Science 271:72–77, 1996.
6. Gros, P., van Gunsteren, W.F., Hol, W.G. Inclusion of thermal motion in crystallographic structures by restrained molecular dynamics. Science 249:1149–1152, 1990.
7. Clarage, J.B., Phillips, G.N. Cross-validation tests of time-averaged molecular dynamics refinements for determination of protein structures by X-ray crystallography. Acta Crystallogr. D50:24–36, 1994.
8. Bonvin, A.M.J., Brunger, A.T. Conformational variability of solution nuclear magnetic resonance structures. J. Mol. Biol. 250:80–93, 1995.
9. De Groot, B.L., Van Aalten, D.M.F., Amadei, S., Berendsen, H.J.C. The consistency of large concerted motions in proteins in molecular dynamics simulations. Biophys. J. 71: 1707–1713, 1996.
10. Rice, L.M., Brunger, A.T. Torsion angle dynamics: Reduced variable conformational sampling enhances crystallographic structure refinement. Proteins 19:277–290, 1994.
11. Brunger, A.T. Free R value: A novel statistical quantity for assessing the accuracy of crystal structures. Nature 355: 472–475, 1992.
12. Deutch, J.M., Madden, T.L. Theoretical studies of DNA during GEL electrophoresis. J. Chem. Phys. 90:2476–2485, 1989.
13. Grønbech-Jensen, N., Doniach, S. Long-time overdamped Langevin dynamics of molecular chains. J. Comp. Chem. 15:997–1012, 1994.
14. Agarwal, R. A new least-squares refinement technique based on the fast Fourier transform algorithm. Acta Crystallogr. A34:791–809, 1978.
15. McDonald, N.Q., Lapatto, R., Murray-Rust, J., Gunning, J., Wlodawer, A., Blundell, T.L. New protein fold revealed by a 2.3-A resolution crystal structure of nerve growth factor. Nature 354:411–414, 1991.
16. Holland, D.R., Cousens, L.S., Meng, W., Matthews, B.W. Nerve growth factor in different crystal forms displays structural flexibility and reveals zinc binding sites. J. Mol. Biol. 239:385–400, 1994.
17. Robinson, R.C., Radziejewski, C., Stuart, D.I., Jones, E.Y. Structure of the brain-derived neurotrophic factor/neurotrophin 3 heterodimer. Biochemistry 34:4139–4146, 1995.
18. Kelly, J.A., Singer, E., Osslund, T.O., Yeates, T.O. Crystallization and preliminary structural studies of neurotrophin-3. Protein Sci. 3:982–983, 1994.
19. Kuriyan, J., Brunger, A.T., Karplus, M., Hendrickson, W.A. X-ray refinement of protein structures by simulated annealing: Test of the method on myohemerythrin. Acta Crystallogr. A45:396, 1989.
20. Navaza, J. AMoRe: An automated package for molecular replacement. Acta Crystallogr. A50:157–163, 1994.
21. Almassy, R.J., Janson, C.A., Hamlin, R., Xuong, N.H., Eisenberg, D. Novel subunit-subunit interactions in the structure of glutamine synthetase. Nature 323:304–309, 1986.
22. Janson, C.A., Almassy, R.J., Westbrook, E.M., Eisenberg, D. Isolation and crystallization of unadenylylated glutamine synthetase from Salmonella typhimurium. Arch. Biochem. Biophys. 228:512–518, 1984.
23. Liaw, S.H., Jun, G., Eisenberg, D. Extending the diffraction limit of protein crystals: The example of glutamine synthetase from Salmonella typhimurium in the presence of its cofactor ATP. Protein Sci. 2:470–471, 1993.
24. Liaw, S.H., Pan, C., Eisenberg, D. Feedback inhibition of fully unadenylylated glutamine synthetase from Salmonella typhimurium by glycine, alanine, and serine. Proc. Natl. Acad. Sci. USA 90:4996–5000, 1993.